systems

MDPI

Article

The Distribution Characteristics and Influencing Factors of Global Armed Conflict Clusters

Mengmeng Hao [1,2], Shijia Ma [1,2], Dong Jiang [1,2], Fangyu Ding [1,2], Shuai Chen [1,2], Jun Zhuo [1,2], Genan Wu [3], Jiping Dong [1,2,*] and Jiajie Wu [1,2,*]

[1] Institute of Geographic Sciences and Natural Resources Research, Chinese Academy of Sciences, Beijing 100101, China; haomm@igsnrr.ac.cn (M.H.); mashijia23@mails.ucas.ac.cn (S.M.); jiangd@igsnrr.ac.cn (D.J.); dingfy@igsnrr.ac.cn (F.D.); chens.20b@igsnrr.ac.cn (S.C.); zhuojun6545@igsnrr.ac.cn (J.Z.)
[2] College of Resources and Environment, University of Chinese Academy of Sciences, Beijing 100049, China
[3] Institute of Spacecraft Application System Engineering, China Academy of Space Technology, Beijing 100094, China; genanw425@126.com
* Correspondence: dongjiping2017@igsnrr.ac.cn (J.D.); wujj.21b@igsnrr.ac.cn (J.W.)

Abstract

Understanding the spatial dynamics and drivers of armed conflict is crucial for anticipating risk and informing targeted interventions. However, current research rarely considers the spatio-temporal clustering characteristics of armed conflicts. Here, we assess the distribution dynamics and driving factors of armed conflict from the perspective of armed conflict clusters, employing complex network dynamic community detection methods and interpretable machine learning approaches. The results show that conflict clusters vary in terms of regional distribution. Sub-Saharan Africa boasts the highest number of conflict clusters, accounting for 37.9% of the global total and covering 40.4% of the total cluster area. In contrast, South Asia and Afghanistan, despite having a smaller proportion of clusters at 12.1%, hold the second-largest cluster area, which is 18.1% of the total. The characteristics of different conflict networks are influenced by different factors. Historical exposure, socio-economic deprivation, and spatial structure are the primary determinants of conflict patterns, while climatic variables contribute less prominently as part of a broader system of environmental vulnerability. Moreover, the influence of driving factors shows spatial heterogeneity. By integrating cluster-level analysis with interpretable machine learning, this study offers a novel perspective for understanding the multidimensional characteristics of armed conflicts.

Keywords: armed conflict clusters; dynamic community detection; interpretable machine learning; driving factors; spatial heterogeneity

check for updates

Received: 30 June 2025
Revised: 30 July 2025
Accepted: 5 August 2025
Published: 7 August 2025

Citation: Hao, M.; Ma, S.; Jiang, D.; Ding, F.; Chen, S.; Zhuo, J.; Wu, G.; Dong, J.; Wu, J. The Distribution Characteristics and Influencing Factors of Global Armed Conflict Clusters. *Systems* **2025**, *13*, 670. https://doi.org/10.3390/systems13080670

Copyright: © 2025 by the authors. Licensee MDPI, Basel, Switzerland. This article is an open access article distributed under the terms and conditions of the Creative Commons Attribution (CC BY) license (https://creativecommons.org/licenses/by/4.0/).

1. Introduction

Armed conflict remains one of the most pressing challenges to global human security [1]. Although the incidence of inter-state war has declined in some regions, the rise in non-state and subnational violence has persisted and intensified, particularly in sub-Saharan Africa, the Middle East, and parts of South Asia. According to the Uppsala Conflict Data Program (UCDP GED 24.1), over 200,000 geographically coded conflict events were recorded globally between 2000 and 2019 [2]. These events exhibit clear patterns of spatial clustering and temporal persistence, revealing the existence of conflict clusters [3].

This widespread and complex nature of conflict highlights not only a threat to the stability of regional societies, but also a systemic challenge to global development goals [4]. Therefore, the study of dynamics and drivers of armed conflicts is becoming increasingly important [5].

With increasing transnational linkages and international interventions, the evolutionary characteristics and drivers of armed conflict have become more complex and diverse [6]. The existing literature has long emphasized structural drivers of armed conflict, including political exclusion, weak institutions, ethnic inequalities, spatial marginalization, etc. [7–9]. Moreover, competition for natural resources is also an important causal factor in some high-conflict areas [10,11]. Other areas have demonstrated that uneven infrastructure, inability to access state services, and remoteness from central authority can create conflicts [12]. Alongside these structural factors, climate variability has emerged as a critical amplifier of violence in recent studies. Although climate is rarely the primary cause of conflict, it is increasingly recognized as a threat multiplier—intensifying risks in areas characterized by livelihood dependence on natural resources, institutional fragility, and social fragmentation [13,14]. For instance, rainfall deficits and heatwaves may trigger livelihood loss and displacement, exacerbating tensions between pastoralists and farmers [15]; moreover, floods can destroy public infrastructure and heighten anti-government grievances in regions with weak disaster response systems [16]. A growing body of empirical research, including meta-analyses [17], confirms that the effects of droughts, floods, and temperature anomalies are nonlinear and highly context-dependent, often intensifying pre-existing grievances rather than initiating new conflict independently. Methodologically, early research largely relied on qualitative case studies or standard multivariate regression models. Seminal works include Collier and Hoeffler's [18] empirical test of the "greed vs. grievance" hypothesis and Hegre et al.'s [19] Cox models of democratization and conflict onset. Nordås and Gleditsch [20] further incorporated geographic proximity in linear regression frameworks. While these approaches identified key statistical relationships, they struggled to capture spatial heterogeneity and nonlinear interactions. Recent years have witnessed a transformation in conflict research into dynamics and drivers, driven largely by the emergence of high-resolution geo-referenced databases, such as UCDP-GED [2], ACLED [1] and PRIO-GRID [21]. These datasets provide unprecedented access to disaggregated records of political violence, enabling scholars to move beyond state-level analysis and investigate conflict dynamics at fine spatial scales. The rise of machine learning methods using fine-resolution spatial data have significantly enhanced the sophistication of conflict driver analysis [13,22].

Moreover, most of the early literature operationalizes conflict either as a binary outcome—the presence (1) or absence (0) of violent events in a grid cell [23,24]—or by using aggregated event-level outcomes such as the number of fatalities [25,26]. These approaches tend to regard conflicts as isolated events, neglecting the spatio-temporal connections between armed conflict incidents. However, armed conflict events often exhibit a high degree of correlation in the spatio-temporal dimension, which is manifested in the clustering and continuity of events in time and space [3]. This has also been demonstrated by several researchers. For instance, Schutte and Weidmann [27] advanced the concept of "conflict diffusion", arguing that violence in neighboring regions is interdependent, thereby challenging the traditional view of conflict as discrete observations. Scholars have also conducted extensive research on spatio-temporal patterns and dynamics of conflicts. Kumarihamy et al. [28] used Getis-OrdGi* statistic combined with Mann–Kendall trend test analysis to identify hot spots and evolving trends in conflict in Sri Lanka from 1989 to 2016; Maswanganye [29] explored spatial clustering along with the spatio-temporal spread of conflict events in Africa from 1997 to 2017. Further, other studies have begun

to quantify conflict dynamics and spatial patterns. Kibris [30] used a split-population bi-probit model to study changes in potential conflict tendency variables affecting the spread of events in Turkey; Tadesse [31] modeled the conflict dynamics in Africa based on the attributes and events of the spatio-temporal ACLED dataset from January 2017 to March 2022, using GIS and robust Poisson regression models to determine hot spots and capture the relationship between various attributes and conflict intensity. Oliveros and Koren [32] proposed a new framework, which provides a new perspective for revealing conflict behavior by creating a conflicting temporal community network (CoDNet), calculating the spatial intensity, diffusion, and concentration of nodes as conflict metrics, and establishing normal associations with variables such as climate pressure. Moreover, studies have increasingly recognized that conflict clusters emerge from diverse mechanisms, with significant variation in their evolution and causal factors. The importance of specific conflict drivers often differs by region due to topography, climate, socio-economic conditions, and governance capacity [33–35].

Despite these advances, three important gaps remain. First, existing studies tend to focus on regional or single-country contexts rather than on the dynamics of conflict in global regions. Second, while scholars have begun to quantify evolutionary trends in conflict occurrence or spread, they have not systematically quantified the relative importance of multidimensional drivers (e.g., geography, socio-economics, climate). Third, there remains a paucity of research on the heterogeneous drivers of different conflict clusters—particularly how such factors vary across regions and spatial scales [31,36]. This study addresses these gaps by adopting a cluster-based perspective to analyze the distribution dynamics and driving factors of armed conflict. Specifically, we construct a conflict network using spatio-temporal proximity on the basis of Oliveros and Koren's work [32] and apply community detection algorithms to extract discrete conflict clusters across the globe. We then quantify multi-dimensional features of these clusters and employ machine learning techniques to assess the relative importance of geographic, socio-economic, and climatic variables in shaping their characteristics and to observe the spatial heterogeneity of variables as drivers. By moving beyond discrete event-level analysis, this study offers a novel framework to evaluate the dynamic and drivers of conflict clusters. This approach allows for a more integrated understanding of armed conflict systems and provides a valuable foundation for context-specific risk mitigation and peacebuilding strategies.

2. Materials and Methods

2.1. Data

2.1.1. Armed Conflict Dataset

The armed conflict data used in this study are sourced from the UCDP Georeferenced Event Dataset (UCDP GED, https://ucdp.uu.se/ (accessed on 3 June 2025)) version 24.1 [2]. UCDP-GED version 24.1 is a publicly available armed conflict dataset with geo-referenced information from 1989 to 2023, which records with at least one person killed in a given location. GED version 24.1 gives the georeferenced coordinates of the conflict events, which facilitates the construction and geo-aggregation of complex networks.

2.1.2. Covariates Dataset

To analyze the evolutionary characteristics of armed conflict clusters, we adopt a multidimensional covariate framework grounded in three interrelated mechanisms: structural vulnerability, external stressors, and diffusion mechanisms. We include historical conflict variables to capture temporal persistence and institutional erosion, as prior violence often increases the probability of recurrence due to weakened governance and unresolved grievances [13]. Then, we incorporate socio-economic indicators such as poverty, pop-

ulation density, and infrastructure access to reflect both grievance formation and state capacity, which shape the opportunity structure for violence [35]. Geographic features, including topography and border proximity, capture mechanisms of diffusion and escalation, whereby violence spreads across adjacent areas with limited state reach or shared ethnic ties [37]. We also integrate climate-related variables such as rainfall deviation and heat extremes to account for environmental shocks that exacerbate livelihood stress, displacement, and inter-group tensions, particularly in resource-dependent contexts [38]. By combining these four domains—conflict history, socio-economic fragility, geographic exposure, and climate stress—our variable design enables a holistic examination of the heterogeneous drivers behind conflict cluster formation and evolution. This integrated approach follows recent calls in the literature for modeling conflict as a complex, spatially embedded, and environmentally contingent phenomenon [13,35,39].

1. Conflict-related variables

History count of armed conflicts before 2000. Areas with a history of high conflict still exhibit low institutional quality and high risk of violence today [40]. This study analyzes the dynamics and drivers of conflict clusters from 2000 to 2019. Therefore, we use the sum of armed conflict history events from 1989 to 1999 in the GED data as the conflict history event static variable based on data availability in the UCDP-GED dataset [2].

2. Socio-economic variables

GDP. Gross domestic product (GDP) serves as a useful indicator for evaluating a country's economic conditions and residents' living standards, reflects national strength, and influences the likelihood of conflict. In this study, we used the global 1 km × 1 km gridded revised real GDP dataset from Scientific Data (GDP, https://www.nature.com/articles/s41597-022-01322-5 (accessed on 3 June 2025)) [41]. The dataset employed a series of methods to unify the scales of DMSP/OLS and NPP/VIIRS images and obtain continuous 1 km × 1 km gridded nighttime light data during the period from 1992 to 2019; subsequently, from a revised real growth perspective, we employed a top-down method to calculate global 1 km × 1 km gridded revised real GDP during the period from 1992 t 2019.

Population. Excessive population growth significantly increases the risk of armed conflict and social instability [42]. We obtained the world gridded population estimates dataset at a resolution of 30 arc (approximately 1 km at the equator) from the WorldPop Open Population Repository (WOPR, https://www.worldpop.org/ (accessed on 3 June 2025)) [43], which uses the mapping approach of Random Forest-based dasymetric redistribution.

Infant mortality rates. Regions with high rates of infant mortality tend to be associated with a higher risk of subsequent conflict and social unrest [44,45]. We obtained data on infant mortality rates from NASA's Socioeconomic Data and Applications Center (SEDAC) (IMR, https://sedac.ciesin.columbia.edu/data/set/povmap-global-subnational-infant-mortality-rates-v2-01 (accessed on 3 June 2025)) [46].

Ethnic diversity. The relationship between ethnic distribution and conflict is similarly strongly correlated. Conflict is more likely to erupt in ethnically clustered areas [47], and the uneven distribution of ethnic groups can also have an impact on the risk of civil war [48]. In this study, we used the geo-referencing of ethnic groups (GREG) dataset, relying on maps and data drawn from the classical Soviet Atlas Narodov Mira (GeoEPR, https://icr.ethz.ch/data/epr/geoepr/ (accessed on 3 June 2025)) [49].

Mineral Resources. Areas rich in mineral resources are more prone to becoming strongholds for armed groups, potentially leading to a significant increase in the frequency and severity of conflicts. The more easily accessible and widely distributed the resources are, the greater the risk of conflict, making regions with extensive and scattered mining sites particularly vulnerable to becoming conflict hotspots [50]. We use the global mining land use

dataset from Scientific Data (Mining, https://doi.pangaea.de/10.1594/PANGAEA.942325 (accessed on 3 June 2025)) [51]. Using visual interpretations of Sentinel-2 images for 2019, more than 34,000 mining locations across the globe were inspected in order to obtain a global-scale dataset; this dataset contained 44,929 polygon features covering 101,583 km^2 of large-scale as well as artisanal and small-scale mining.

3. Geographical environment

Natural disaster hotpots. Natural disasters (floods, droughts, storms) can prolong the duration of civil wars [52] and increase the likelihood of violent civil wars occurring, especially when they cause severe economic damage [53]. In this study, the Global Multihazard Frequency and Distribution Dataset was used, which reflects the frequency and distribution of multihazard events. This dataset is a 2.5 min gridded dataset that presents a simple multi-hazard index based on the sum of decile values for individual hazards (GMFD, https://catalog.data.gov/dataset/global-multihazard-frequency-and-distribution (accessed on 3 June 2025)) [54].

Vegetation index. Research has found an association between conflict and positive vegetation growth [55]. We acquired the Normalized Difference Vegetation Index (NDVI) form Distributed Active Archive Center (DAAC) (NDVI, https://daac.ornl.gov/VEGETATION/guides/Global_Veg_Greenness_GIMMS_3G.html (accessed on 3 June 2025)) [56]. NDVI was based on corrected and calibrated measurements from Advanced Very-High-Resolution Radiometer (AVHRR) data with a spatial resolution of 0.0833 degrees and global coverage for 1982 to 2022.

Urban accessibility. The transportation hub is often the target place that strategists must contend for due to the key role of control territories. Roads facilitate the transmission of violence to new locations, and can also intensify competition for limited military resources between nearby battlefronts [57]. In this study, various urban accessibility static variables provided by the PRIO-GRID dataset were used (PRIO-GRID, https://grid.prio.org/#/download (accessed on 3 June 2025)) [21], including variables such as distance to the border, distance to the capital city and mean travel distance to the nearest urban center, which are gridded data with a $0.5^\circ \times 0.5^\circ$ resolution, matching the specifications of the other covariates. We also obtained the road density dataset from The Global Roads Inventory Project (GRIP, https://www.globio.info/download-grip-dataset (accessed on 3 June 2025)) [58], city land use data from the PANGAEA repository (PANGAEA, https://doi.org/10.1594/PANGAEA.921846 (accessed on 3 June 2025)) [59] and the critical infrastructure (CI) dataset from Scientific Data (CI, https://www.nature.com/articles/s41597-022-01218-4 (accessed on 3 June 2025)) [60].

Topography. Geographic location and terrain features such as ruggedness can affect the occurrence and distribution of conflicts [61]. We acquired the mountain range dataset from Scientific Data, which provided a new inventory of 8616 mountain ranges developed under the auspices of the Global Mountain Biodiversity Assessment (GMBA, https://www.nature.com/articles/s41597-022-01256-y (accessed on 3 June 2025)) [62]; we also obtained global water cover data from the PRIO-GRID dataset with a $0.5^\circ \times 0.5^\circ$ resolution, matching the specifications of the other covariates.

4. Climatic variability

Precipitation Anomaly. Studies have found that both deficits and excesses of precipitation can have an impact on different types of social conflict events [63], and that precipitation fluctuations are significantly associated with an increased risk of conflict, controlling for long-term averages [64]. For example, reduced precipitation following the 1998 El Niño increased the risk of conflict in Ethiopian and Kenyan communities, which, in turn, threatened social stability [65]. CRU TS is one of the most widely used

climate datasets which is produced by the UK's National Centre for Atmospheric Sciences (NCAS, https://crudata.uea.ac.uk/cru/data/hrg/ (accessed on 3 June 2025)) [66]. In this study, we compute a standardized precipitation index to represent deviations from average precipitation, using 0.5° × 0.5° monthly precipitation data downloaded from CRU.

Temperature Anomaly. Temperature variability is associated with conflict. Extreme temperature events may trigger more armed violence [67]; rising temperatures are strongly associated with increased conflict rates [68,69], especially in hotter regions [70]. In this study, the standardized temperature index is used to measure the deviation from the mean temperature. We obtained the 0.5° × 0.5° monthly mean surface temperature dataset from the Global Historical Climatology Network (GHCN, https://psl.noaa.gov/data/gridded/data.ghcncams.html (accessed on 3 June 2025)) [71], and calculated the annual mean surface temperature data and the annual standardized temperature index.

To achieve unified modeling and spatial-temporal analysis, the following preprocessing was performed: All data were geo-aggregated at a latitude and longitude resolution of 0.5° × 0.5°, with each grid cell corresponding to about 55 km × 55 km (equatorial region) to balance geographic accuracy with computational feasibility. Point objects were assigned to the nearest grid center. Raster type variables were resampled to a grid size of 0.5° × 0.5°, with the annual mean as the data value for each grid cell. All datasets were tested for outliers to reduce the impact of extreme values. Missing point object records for a grid-year combination were considered conflict absences and filled with zeros. Missing values in auxiliary variables, such as climate or population data, were filled in by regional mean interpolation. Datasets were merged by grid number and time label to construct complete spatio-temporal panel data.

2.2. Extraction of Armed Conflict Clusters and Feature Calculation

2.2.1. Construction of Armed Conflict Event Network Based on Spatio-Temporal Proximity

By constructing spatio-temporal conflict networks based on proximity and timing [72,73], and applying community detection algorithms, we can identify conflict clusters that offer richer analytical units than individual events. Wu [74] used near-repetition analysis to identify significant clustering patterns by counting the spatio-temporal distances between armed events, thereby determining reasonable spatio-temporal ranges, and found that there was a significant risk of conflict in different regions within a spatial range of 300 km and within a time window of 720 days after the original conflict occurred. Therefore, the spatial threshold of 300 km and the time threshold of 720 days (about two years) were selected to construct the conflict network [27,32,33,57,75,76]. Firstly, each conflict event was identified as a node in the network, with the attributes of the node including key information such as the specific location of the event when it occurred and the type of the event. Next, the connectivity between nodes was determined based on the results of the spatio-temporal proximity measure. In other words, if the spatial distance between two conflict events is less than or equal to 300 km and the time interval between their occurrences is within 720 days, then an edge is created between these two nodes to represent the spatio-temporal proximity relationship between them. Finally, all nodes and edges were combined to form a complete conflict network. This network structure visualizes spatio-temporal correlations and interactions between conflict events.

The multi-year network formed through the construction of spatio-temporally neighboring geo-conflict event networks is both complex and extensive. Given the sheer number of nodes and edges, as well as their often-irregular connections, it becomes highly challenging to directly extract meaningful communities from such a network. To solve this problem, we adopted a geo-aggregation approach to simplify the complex spatio-temporal proximity geo-conflict event network formed in the previous step by combining the geo-conflict event

network with a geographic grid. We matched the network nodes, i.e., conflict events, in the geo-conflict event network to the corresponding grid cells based on their geographic locations. If at least one pair of associated conflict events exists between two grid cells, then an edge exists between them, and the number of pairs of geo-conflict events existing between the grid cells indicates the strength/weight of spatial connection between the grid cells. In this paper, we chose the $0.5^\circ \times 0.5^\circ$ grid cell as the base grid cell based on the availability of the datasets. Geo-aggregation greatly simplifies the complex network of geo-conflict events, allowing otherwise difficult-to-recognize spatial patterns to be clearer without discarding any closely related pairs of conflict events.

2.2.2. Detection of Armed Conflict Clusters

According to Schutte and Weidmann [27], conflict events are not randomly distributed but tend to cluster in space and time, driven by processes such as tactical imitation, informational spillover, and strategic signaling. These dynamics give rise to coherent conflict clusters that reflect both the intensity and continuity of violence. In parallel, the contagion and escalation framework proposed by Buhaug and Gleditsch [33] suggests that violence spreads through cross-border linkages (contagion) and intensifies through local feedback loops (escalation). Together, these theories imply that conflict evolves through interacting spatial processes that transcend administrative boundaries. Our approach operationalizes these insights by applying community detection algorithms to extract empirically grounded clusters of violence. These clusters serve as the units of analysis to assess how geographic, socio-economic, and climatic factors jointly influence the dynamics of violence, allowing us to move beyond discrete event analysis and better capture the multi-scalar, networked nature of modern conflict systems. To identify clusters of conflict within the dynamic spatio-temporal network, we adopted the Louvain community detection algorithm. This method is particularly well-suited for large-scale and evolving networks due to its computational efficiency, hierarchical detection capability, and ability to operate without a priori specification of the number of communities [77–79]. These characteristics make it especially appropriate for conflict systems, which are often sparse, temporally irregular, and spatially fragmented. This approach has seen broad application in identifying localized conflict patterns, including civil war groupings [32], violence-prone areas in Bangladesh [80], and conflict dynamics related to displacement in Somalia [81]. To assess the robustness and reliability of our choice, we compared the Louvain algorithm with two alternative methods widely used in the literature—Greedy Modularity Optimization and Asynchronous Label Propagation (LPA)—using sensitivity analysis on resolution parameters (as shown in Appendix A Table A1) to test the impact on community granularity and modularity. The LPA algorithm has no resolution parameter. The modularity value mainly depends on the community distribution of nodes in the network—that is, the community division of the network. It can be used to quantitatively measure the quality of community division of the network. The closer its value is to 1, the stronger the community structure divided by the network is, and the better the division quality. Considering that the modularity and community size median is greater than 5 after excluding communities with grid number less than 5, we choose louvain_communities (resolution = 1) as the community detection algorithm. The algorithm operates in two main phases. Initially, each node is treated as a separate community. Then, for every node, the algorithm evaluates the potential modularity increase that would result from shifting the node into each of its neighboring communities. The node is moved only if doing so yields a positive modularity gain; oth-

erwise, it stays in its current community. The change in modularity when transferring an individual node into another community is computed using the following equation:

$$\Delta Q = \frac{k_{i,in}}{2m} - \gamma \frac{\sum tot \cdot k_i}{2m^2} \quad (1)$$

where m is the size of the graph, $k_{i,in}$ is the sum of the weights of the links from i to nodes in z, k_i is the sum of the weights of the links incident to node i. $\sum tot$ is the sum of the weights of the links incident to nodes in z and γ is the resolution parameter. The first phase continues until no individual move can improve the modularity. The second phase consists of building a new network whose nodes are now the communities found in the first phase. To achieve this, the weights of the links between the new nodes are given by the sum of the weight of the links between nodes in the two corresponding communities. Once this phase is complete, it is possible to reapply the first phase, creating bigger communities with increased modularity. The two phases given above are executed until no modularity gain is achieved (or is less than the threshold).

2.2.3. Calculation of Armed Conflict Cluster Indicators

To better capture the structural and dynamic characteristics of armed conflicts, we selected four core indicators to represent the features of conflict clusters, namely the number of conflicts, average intensity, dispersion, and intra-connectivity. We took the conflict cluster as the unit of analysis, with the four indicators of each conflict cluster serving as the dependent variables for subsequent modeling [32].

1. Number of conflicts—operationalized as the number of conflict events between conflict cell-years $\left(c_z^{(t)}\right)$ within a given cluster z during a given year $t\left(num_z^{(t)}\right)$.

$$sum_z^{(t)} = \sum_i num_z^{(t)} \quad (2)$$

This indicator allows us to measure the total number of conflict events that occurred in all cells in a particular conflict cluster in a given year, which indicates the frequency of conflict events in a conflict cluster and provides a visual indication of the intensity of conflict in a conflict area.

2. Average intensity—operationalized as the average degree between conflict cell-years $\left(c_z^{(t)}\right)$ within a given cluster z during a given year t. This variable captures the average activity level of a given conflict node (cell-year).

$$k_z^{(t)} = \frac{2m_z^{(t)}}{n_z^{(t)}} \quad (3)$$

This indicator captures how destabilizing it is to be around a particular conflict cell in a given year, which actually reflects the likelihood that conflict will spread to other parts of the cluster in space and time, i.e., how unstable inside a conflict cluster.

3. Dispersion—operationalized as the number of active cell-month (i.e., that experienced conflict events) during a given year t within a cluster z.

$$n_z^{(t)} = \left| c_z^{(t)} \right| \quad (4)$$

The indicator reflects how many cell-months experiencing conflict in a given year, which captures the influence extent of conflict within a conflict cluster.

4. Intra-connectivity—operationalized as the number of links between conflict cell-years $\left(c_z^{(t)}\right)$ in each cluster z. i.e., the number of edges $\left(e_z^{(t)}\right)$ in the cluster.

$$m_z^{(t)} = \sum_i e_z^{(t)} \tag{5}$$

This indicator allows us to measure the level of activity within a conflict cluster, i.e., how many cells in a given conflict cluster are in conflict at the same time period in a given year. The higher the intra-connectivity, the more overall conflict the corresponding cluster experiences in time and space, and the easier it is for conflicts to move and spread across locations.

2.2.4. Analysis of Influencing Factors of Armed Conflict Clusters

To simulate the relationship between armed conflict cluster indicators and potential influencing factors, this study employs Random Forest regression (RF), a non-parametric machine learning method that can accommodate complex, nonlinear interactions between variables. RF is a powerful ensemble learning method [82], which obtains the final continuous prediction by calculating the average of the outputs of all the decision trees, which can increase the diversity of the forest and reduce the risk of overfitting and enhance the generalizability of the model [83]. For each of the four dependent variables, a separate RF model is trained using the cluster-level data. Covariate elements mainly include the history of armed conflicts, socio-economic conditions, geographical environment, and climate change factors. Specific indicators are introduced in the data section. To reduce redundancy and multicollinearity, we applied Pearson correlation filtering. Pairs of variables with a correlation coefficient >0.9 were identified, and one variable from each pair was dropped. This step ensures model interpretability and reduces noise. Each RF model was trained using an 80/20 train–test split on the cluster-level dataset. We used the RandomForestRegressor implementation from scikit-learn with a fixed random seed of 42 to ensure reproducibility. To ensure robust performance, hyperparameter tuning was conducted using RandomizedSearchCV with 100 iterations over a predefined parameter space, including the number of trees (n_estimators), tree depth (max_depth), feature selection strategy (max_features), and regularization parameters (min_samples_split, min_samples_leaf, ccp_alpha). The model was evaluated using a 10-fold cross-validation scheme with the coefficient of determination (R^2) as the scoring metric. The loss function optimized during training was the mean squared error (MSE), and parallel computation was enabled via n_jobs = -1 to enhance efficiency. This approach allowed us to identify the best-performing model configuration while minimizing overfitting and maximizing generalizability across different conflict indicators.

To interpret the machine learning results and analyze the spatial heterogeneity of covariate importance, we adopted the SHapley Additive Explanations (SHAP) framework. SHAP feature importance is based on the concept of Shapley values introduced in cooperative game theory [84]. Consider a game with a set of players denoted by the set $D = \{1, ., d\}$, where d is the total number of players. They can form coalitions $K \subseteq D$. We define a value function $\nu : 2^d \to R_+$, where 2^d denotes the set of all possible coalitions of players. The function ν assigns each subset of players a non-negative true number corresponding to their payoffs. Player j is paid as follows:

$$\phi_j(\upsilon) = \sum_{K \subseteq P \setminus \{j\}} \frac{|K|!(|D| - |K| - 1)!}{|D|!} [\upsilon(K \cup \{j\}) - \nu(K)] \tag{6}$$

where the difference between the value functions quantifies the marginal contribution of the j-th player in coalition K. Assuming they cooperate, the SHAP value allows rewards to

be allocated fairly among players. SHAP offers a model-agnostic, locally faithful method for decomposing predictions into feature-level contributions. SHAP generates a value for each input feature (also known as a SHAP value) that indicates each feature's marginal contribution [37]. For each Random Forest model, we calculated the mean of the absolute SHAP values across all clusters for each explanatory variable. This value reflects the average magnitude of influence that a variable has across the dataset regardless of direction. We used this score as the basis for feature importance ranking, offering a robust and interpretable measure of each variable's impact. SHAP values were mapped spatially at the cluster level. Each conflict cluster retained an associated variable's SHAP score. These values were projected onto geographic maps using the grid distribution of clusters, yielding visualizations of feature importance. This approach highlighted regions where these variables were major explanatory drivers of conflict clusters or played minimal or negligible roles.

3. Results

3.1. The Spatio-Temporal Evolution Characteristics of Armed Conflict Clusters

To compare the differences between armed conflicts clusters in different regions, we divided the map into six regions for comparative analysis (as shown in Figure 1): Latin America, Southeast Asia, South Asia and Afghanistan, the Middle East, sub-Saharan Africa, and Europe and North Africa. A total of 124 conflict clusters were identified globally between 2000 and 2019, covering 5250 grid cells. sub-Saharan Africa hosts the largest number of clusters, which is 47, covering 2120 grid cells; this is followed by Latin America, which has 24 clusters, and Southeast Asia, which has 16 clusters. Regions such as Europe and North Africa exhibit fewer clusters, concentrated in specific locales like Algeria and Libya. The extracted clusters vary not only in number but also in spatial scale. Despite the small number of clusters in South Asia and Afghanistan, the grid cells are second in terms of coverage (953 grids), indicating a greater concentration of conflict. The Latin America cluster covers 930 grids, accounting for 17.7% of the conflict area, ranking third. High-density agglomerations are also observable across Nigeria, Colombia, and the Syrian–Iraqi border zone.

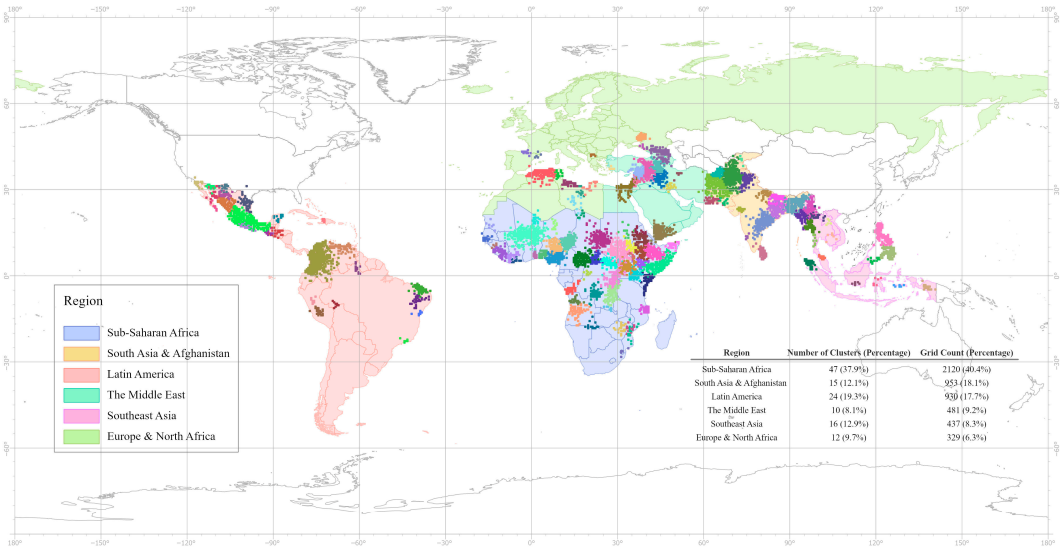


Figure 1. The spatial distribution of armed conflict clusters. Distribution of conflict clusters and their grid coverage across six world regions between 2000 and 2019. The different colors of the points represent different clusters of conflict events from 2000 to 2019.

In order to analyze the overall changes in clusters from 2000 to 2019, we take the cluster distributions in 2000, 2010 and 2019 as an example to observe the distribution, number and coverage of clusters (as shown in Figure 2). In sub-Saharan Africa, the total number of conflict clusters decreased from 33 in 2000 to 25 in 2010, then rebounded to 35 in 2019. The number of grids covered showed the same trend, decreasing from 312 to 213 and further increasing to 564. Conflict clusters were mainly distributed in Central Africa, Northern East Africa, Southern West Africa and Central Africa. The number of clusters in South Asia and Afghanistan did not change much overall, but the number of grids occupied was the highest in 2010, accounting for 38.4%. Clusters are mainly distributed in Palestine, Afghanistan, Nepal and Eastern India. The number of clusters and grid coverage in Latin America has been increasing from 2000 to 2019, but the grid coverage has slightly shrunk in 2010. Clusters were mainly concentrated in Colombia and Mexico. The number of conflict clusters in the Middle East, Southeast Asia, Europe and North Africa changed little overall, with regional concentrations in Syria–Iraq region, northern Algeria, northwestern Thailand and Philippines, but the cluster coverage in the Middle East has increased from 43 in 2000 to 232 in 2019.

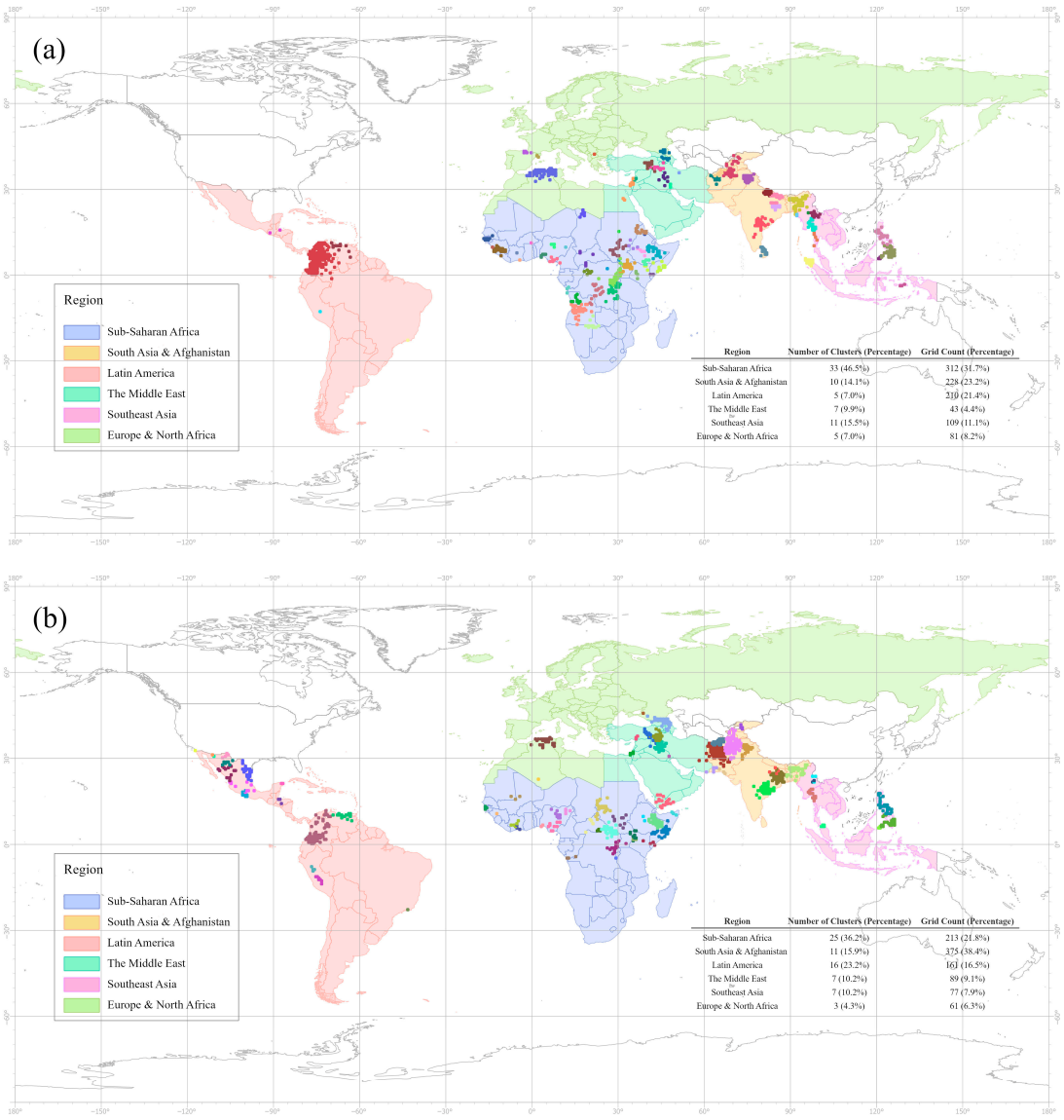


Figure 2. *Cont.*

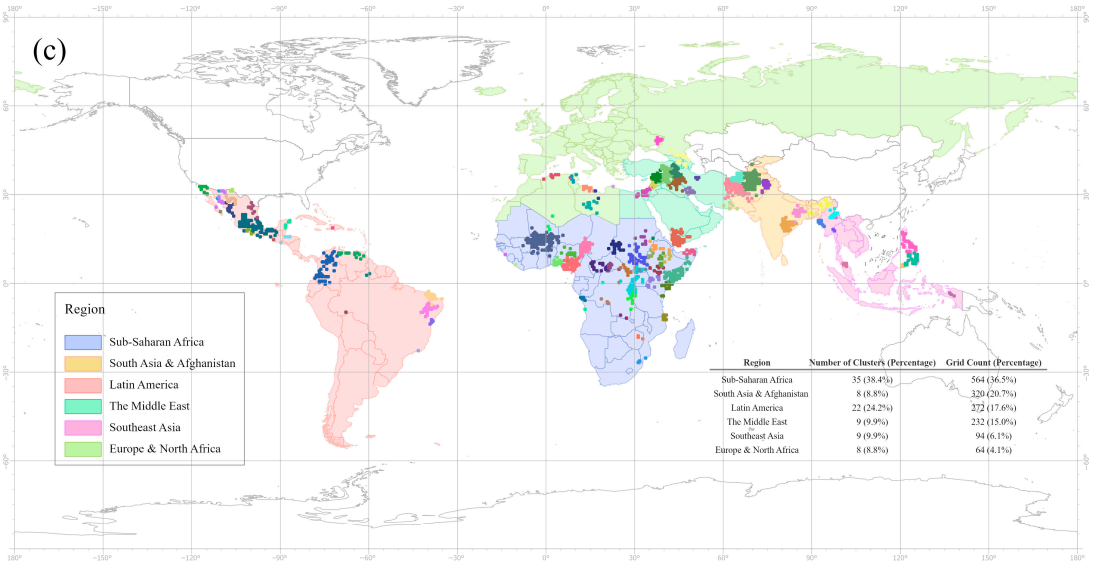


Figure 2. The spatial distribution of armed conflict clusters of 2000, 2010 and 2019. Global distribution of conflict clusters and their grid coverage across six world regions in (**a**) 2000, (**b**) 2010, and (**c**) 2019.

To further examine the temporal characteristics of these clusters, we tracked the annual averages of four core indicators across time in six regions: number of conflicts, average intensity, dispersion, and intra-connectivity (as shown in Figure 3). Latin America shows obvious fluctuation in the number of conflicts, which is lower than that of other regions; after 2016, the average intensity, dispersion and interconnection index rose simultaneously, showing the characteristics of gradual escalation and proliferation linkage of conflicts in Latin America after 2016. The number of conflicts in South-East Asia is not high compared with other regions vertically; the other three indicators also fluctuate, but the overall trend is decreasing, indicating that the conflict area in South-East Asia is more stable and dispersed. The number and average intensity of conflicts in South Asia and Afghanistan have steadily increased, but the fragmentation index and internal connectivity index have declined since 2010, indicating that conflicts in South Asia and Afghanistan are characterized by increasing intensity and concentration. In contrast, there were few conflicts in the Middle East region before 2010, but they began to rise during 2010–2014 and declined after reaching a peak, but remained at a very high level. The other three indicators changed simultaneously, indicating that large-scale conflicts occurred in the Middle East region in 2010, and that conflicts gradually spread and escalated; however, the conflicts then weakened, showing characteristics of sporadic distribution. The overall number of conflicts in Europe and North Africa is at a lower level vertically than in other regions; in 2013, the number and average intensity of conflicts increased sharply but declined rapidly, indicating that large-scale conflicts occurred in 2013 and showed a trend of spreading and escalating, but gradually weakened after 2014. The number of conflicts in sub-Saharan Africa is on a steady upward trend, but at a moderately low level compared to other regions; the other three indicators are also on a steady upward trend, indicating that conflicts in sub-Saharan Africa are gradually increasing and spreading to more areas.

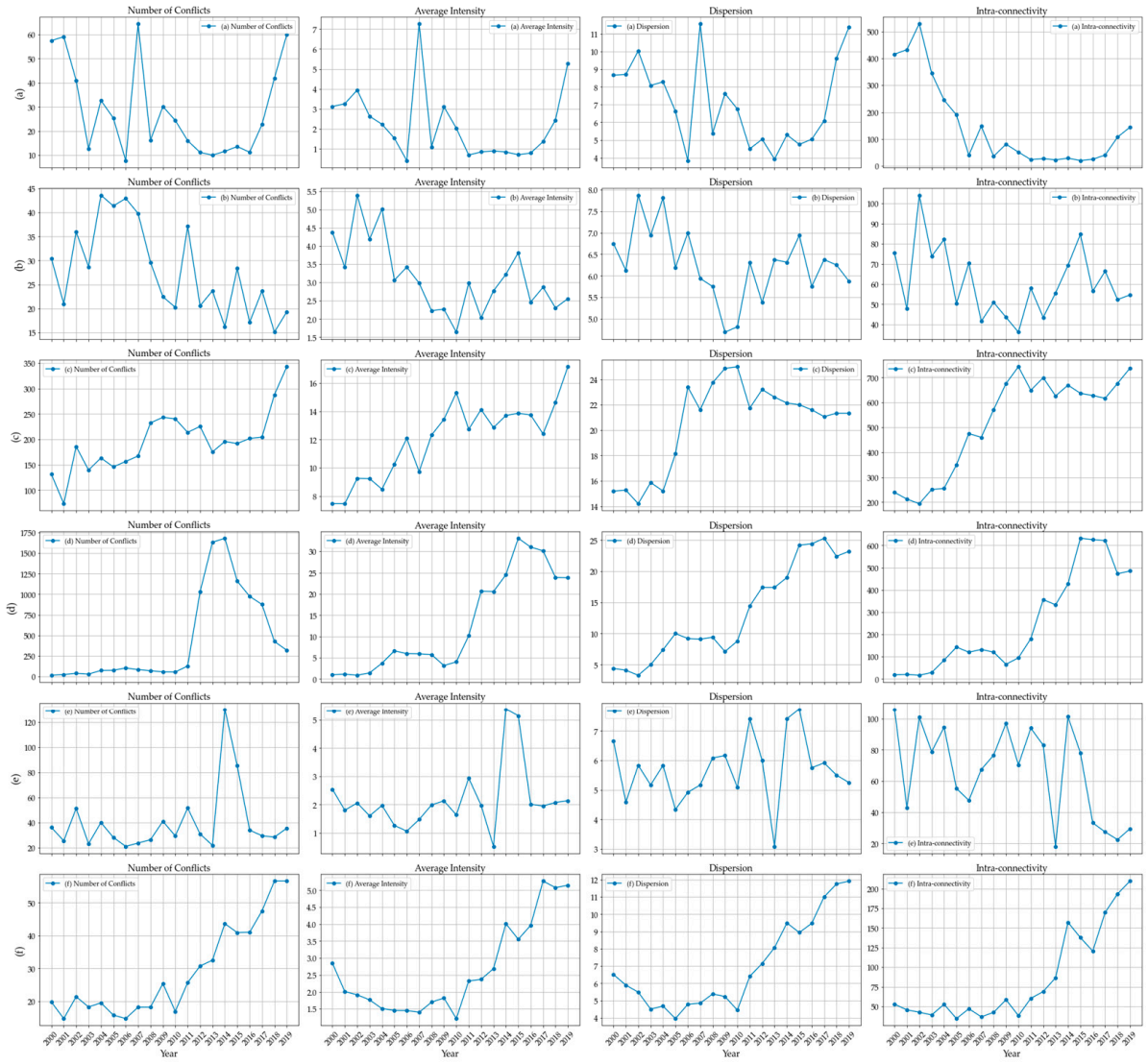


Figure 3. Yearly average dynamics of four conflict metrics—number of conflicts, average intensity, dispersion, and intra-connectivity for six regions. Panels (**a**,**f**) represent six regions, respectively: (**a**) Latin America; (**b**) Southeast Asia; (**c**) South Asia and Afghanistan; (**d**) the Middle East; (**e**) Europe and North Africa; (**f**) sub-Saharan Africa; these illustrate distinct temporal profiles and structural evolution patterns of conflict clusters.

3.2. Modeling Results of Random Forest Regression

Before modeling, we applied Pearson correlation filtering to detect multicollinearity. We dropped one pair of variables with a correlation coefficient > 0.9; the correlation coefficient matrix is shown in Supplementary Materials Figure S15. To evaluate the performance of different key features on conflict dynamics, we employed Random Forest regression models across four conflict-related indicators. Model parameters were optimized using a randomized search over hyperparameter space, and 10-fold cross-validation (CV) was used to assess generalizability. The results are summarized as follows: For the number of conflicts, the optimal model utilized 200 trees with a maximum depth of 15, a log2 feature sampling strategy, and no bootstrap sampling. The model achieved a 10-fold CV mean R^2 of 0.704 ($\pm$0.166), indicating strong generalizability power with moderate variance across folds. In the case of average intensity, the best model shared the same hyperparameters as the incidence model (200 trees, log2 features, depth 15, no bootstrap), and yielded an even higher CV R^2 of 0.792 ($\pm$0.062), demonstrating stable and accurate

model performance for conflict instability. The dispersion of conflict events was modeled most effectively using a shallower ensemble of only 50 trees, with a maximum depth of 20 and sqrt feature selection. This configuration produced the highest accuracy among all outcomes, with a CV R^2 of 0.863 ($\pm$0.061). For the intra-connectivity index, a more regularized model with 50 estimators, deeper trees (depth = 30), and stronger constraints on node splitting (min_samples_split = 5, min_samples_leaf = 2) was favored. This setup resulted in a CV R^2 of 0.811 ($\pm$0.160), reflecting a high overall fit with some variability across partitions. These results suggest that the spatial and structural predictors used in the model possess substantial explanatory power across all four conflict metrics, particularly for capturing spatial dispersion and intensity patterns. The consistently high cross-validated R^2 values confirm the robustness of the Random Forest approach in modeling complex conflict-related dynamics.

3.3. The Influencing Factors of the Armed Conflict Cluster Indicators

To further interpret the learned models, SHAP (SHapley Additive exPlanations) values were computed to quantify the contribution of each feature to the models. Figure 4 summarizes both the top 10 features by mean absolute SHAP value and their aggregated importance by thematic group. To improve the interpretability of the model, in addition to the SHAP values, we also present partial dependence plots for each variable to further illustrate the relationship between the model predictions and individual variables, as shown in Supplementary Materials Figures S16–S19.

For feature group contribution, geographical factors (e.g., distance to border/state/capital, disaster hotpots, urban accessibility) accounted for the largest share of explanatory power in all models, ranging from 33.71% to 38.96%. Socio-economic features, such as population, GDP, infant mortality rate (IMR), and ethnic composition, contributed between 27.08% and 37.64%, reinforcing the relevance of developmental inequalities. Conflict-related variables (primarily Hist_con_cnt) provided moderate explanatory value, especially in the dispersion and intra-connectivity models. Climatic variables (SPI and STI) had comparatively lower standalone influence (typically <10%), yet they consistently appeared among the top 10 features, highlighting a secondary but non-negligible role of climatic stressors in shaping conflict dynamics. Across all four outcome variables, historical conflict exposure (Hist_con_cnt) consistently emerged as the most influential feature, underscoring the persistence and path dependency of violence in conflict-prone areas. This dominance was particularly pronounced in models predicting conflict incidence, intensity, and dispersion. Vegetation coverage (NDVI) and ethnic group heterogeneity (Ethnic_groups) were also among the most impactful predictors across outcomes. NDVI, as a proxy for environmental productivity, exhibited strong predictive power for both conflict incidence and intensity, potentially capturing resource-based grievances. Ethnic fractionalization was the second most important driver of dispersion and intra-connectivity, suggesting that social fragmentation exacerbates spatial diffusion of violence. In terms of the number of conflict events, GDP, population and other socio-economic variables also ranked first, indicating that the deterioration of socio-economic conditions also produces conflicts. STI also ranked highly for the average intensity indicator, indicating that extreme temperatures can also exacerbate instability in conflict areas. Geographic variables, such as dispersion and intra-connectivity indicators, distance to boundaries, and global multihazard frequency, also ranked highly, indicating that geographic variables plays a greater role in conflict coverage and linkage.

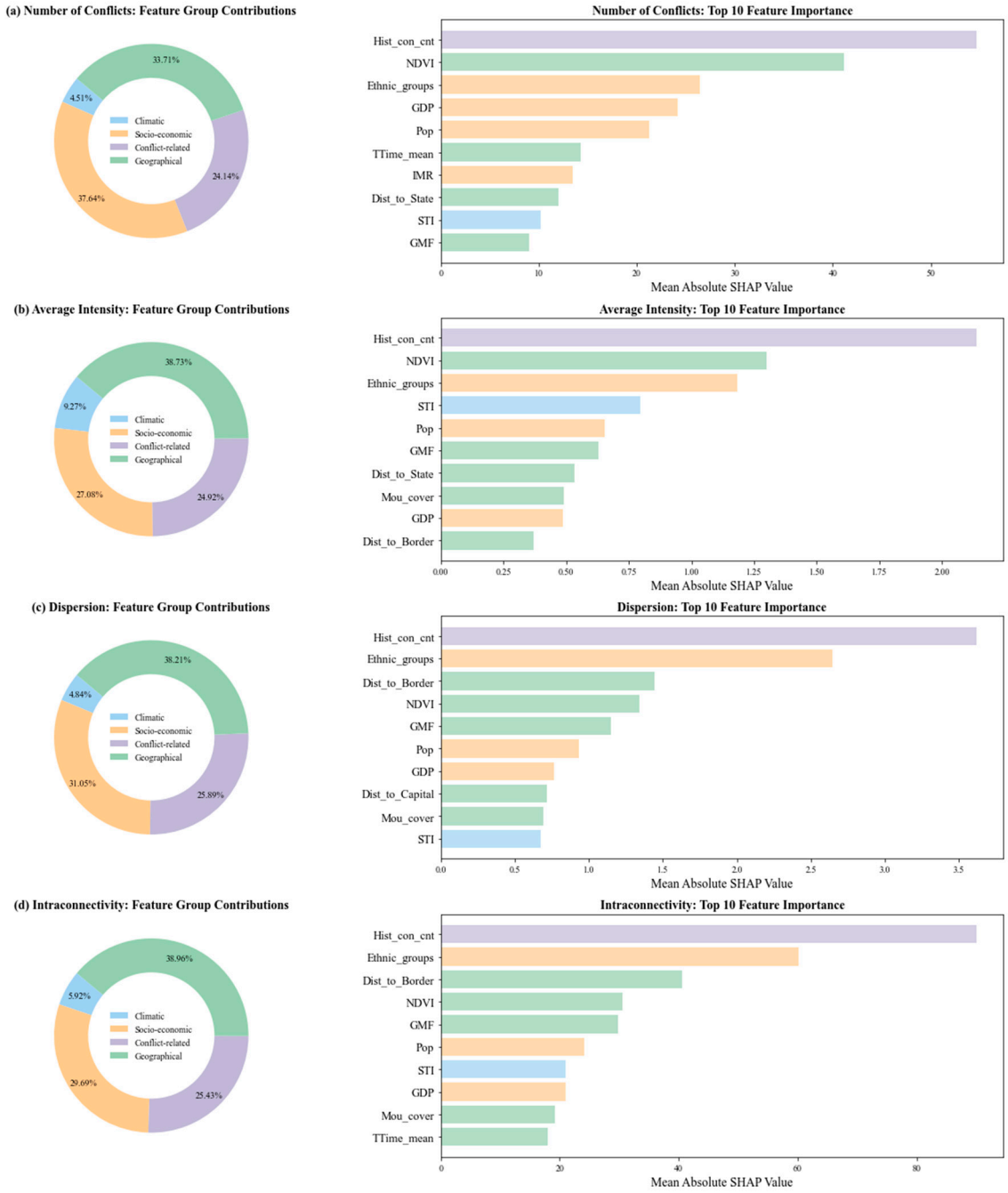


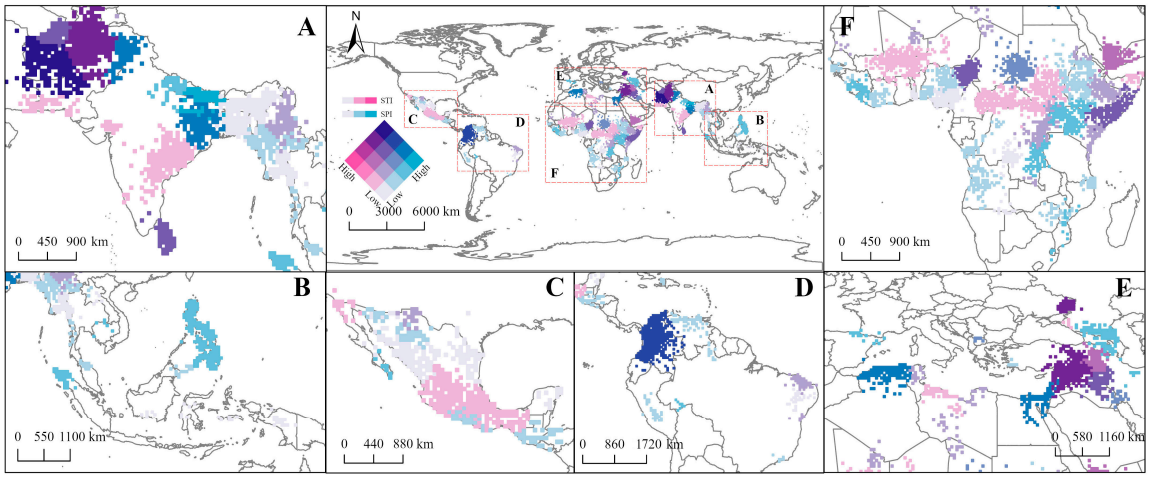
Figure 4. Feature group contributions and feature importance ranking for different armed conflict cluster indicators. Panels (**a**–**d**) represent the modeling results of the four indicators of conflict clusters, respectively: (**a**) number of conflicts; (**b**) average intensity; (**c**) dispersion; (**d**) intra-connectivity. The variables in the figure are denoted as follows: (1) GDP: gross domestic product; (2) Pop: population; (3) IMR: infant mortality rates; (4) Ethnic_groups: ethnic groups; (5) STI: standardized temperature index (STI); (6) GMF: global multihazard frequency; (7) Dist_to_Capital: distance to the capital city; (8) Dist_to_Border: distance to the border; (9) Dist_to_State: distance to the closest country anywhere; (10) TTime_mean: mean travel time to the nearest urban center; (11) NDVI: global vegetation greenness; (12) Mou_cover: mountain range; (13) Hist_con_cnt: the history count of armed conflicts before 2000.

3.4. Analysis of Spatial Heterogeneity of Covariate Effects

Through interpretable machine learning, we also recorded differences in the impact of influencing factors on different clusters. This section uses climate variation as an example to illustrate the spatial heterogeneity of the influencing factors of the cluster. To investigate

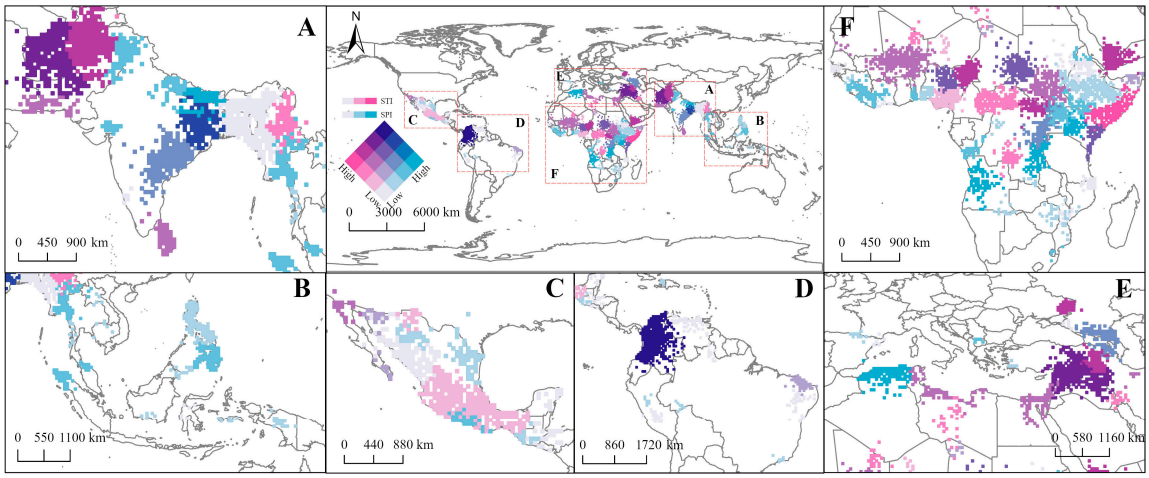
the spatial variation in climate variation–armed conflict linkages, we visualized the SHAP-based spatial importance of two climatic variables—standardized precipitation index (SPI) and standardized temperature index (STI)—in driving each of the four conflict cluster characteristics (as shown in Figure 5). These bivariate maps present a nuanced picture of how climate stressors operate across space, illustrating that climate does not exert a uniform effect on armed conflict, but rather shows significant heterogeneity in both direction and magnitude depending on regional context and conflict dimension. We have also provided spatial maps of other variables base on SHAP (Supplementary Materials Figures S1–S14).

The spatial differentiation of conflict clusters influenced by climate anomalies shows significant regional variability. Overall, South Asia—particularly the northern Indian subcontinent near the Pakistan border—as well as Afghanistan and large areas of Syria and Iraq, exhibited high values across all four structural indicators (frequency, intensity, dispersion, and interconnectivity) under both high standardized temperature index (STI) and high standardized precipitation index (SPI). These regions, shown in deep purple, indicate that conflict activity is jointly driven by extreme temperature and precipitation anomalies. Similar dual climate influence patterns are visible in parts of West Africa (e.g., Guinea, northeastern Nigeria), East–Central Africa (eastern and southern Sudan, Ethiopia), and Latin America (notably Colombia), suggesting that both temperature and precipitation extremes are closely linked to the intensity and spread of armed conflict in these areas. In contrast, temperature-dominant regions such as western Myanmar, Libya, and the Central African Republic are characterized by high STI (pink shading) with low SPI signals (lack of blue hues), indicating that heat-related stress is the primary climatic driver of conflict escalation in these areas. Conversely, precipitation-driven regions—marked in bluish hues—include Nepal, northern Algeria, Kenya, the Democratic Republic of Congo, and the Philippines. These areas show strong SPI influence while STI remains relatively low, implying that anomalous rainfall patterns act as a key triggering factor for conflict emergence. Finally, heterogeneity exists in how different indicators respond to climate anomalies. For example, in southern Mexico and Guatemala, conflict frequency and average intensity are strongly affected by temperature anomalies, whereas interconnectivity is primarily influenced by precipitation, and dispersion reflects a combined effect. This suggests that while heat stress may initiate conflict, its escalation and spread may depend on concurrent or subsequent precipitation anomalies.

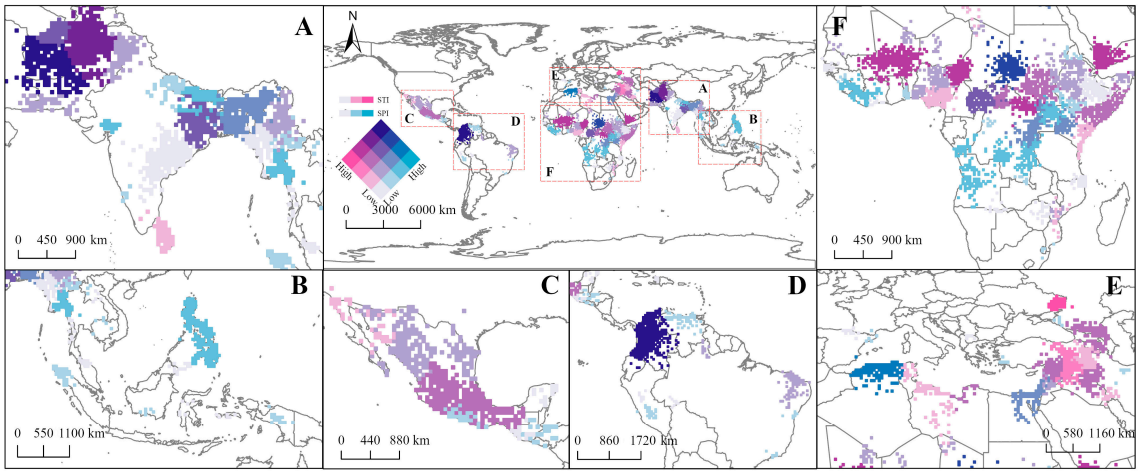


(**a**)

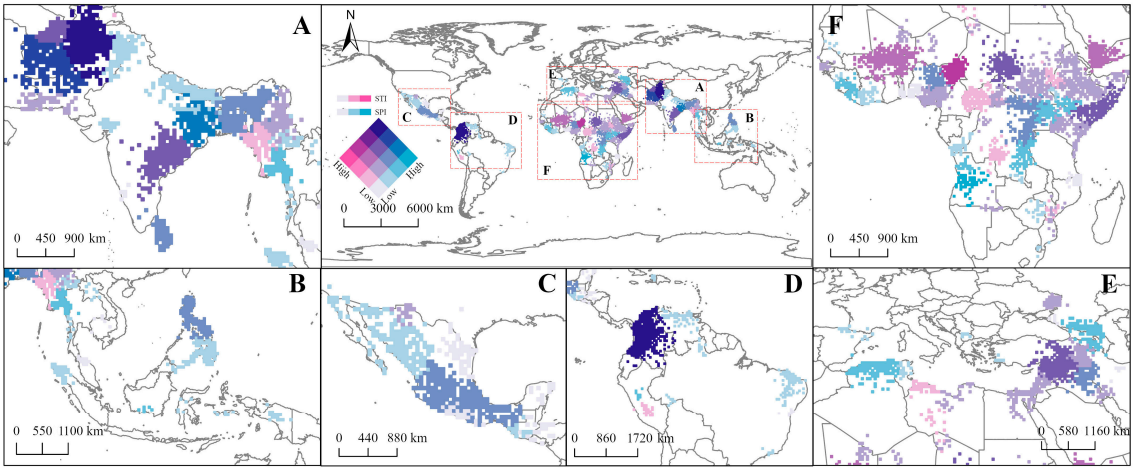
Figure 5. *Cont.*



(**b**)



(**c**)



(**d**)

Figure 5. The spatial heterogeneity of the impact of climate variation on armed conflict clusters. Panels (**a**–**d**) represent the spatial distribution of SHAP values for SPI and STI on four conflict indicators, respectively: (**a**) number of conflicts; (**b**) average intensity; (**c**) dispersion; (**d**) intra-connectivity. Blue indicates higher importance of SPI, pink indicates higher importance of STI, and purple denotes strong dual influence. Insets (A–F) correspond to regional conflict zones: (A) South Asia and Afghanistan; (B) Southeast Asia; (C,D) Latin America; (E) the Middle East, Europe and North Africa; (F) sub-Saharan Africa.

4. Discussion

This study shifted the analytical focus from isolated conflict events to spatio-temporally coherent conflict clusters. By integrating community detection, feature-based machine learning, and spatial interpretability, this analysis provides a multidimensional view of the dynamic and drivers of armed conflict clusters. The discussion below synthesizes the key findings, placing them within the context of existing scholarship and reflecting on the broader theoretical and policy implications.

The results demonstrate the value of a cluster-based framework for analyzing the dynamics and drivers of armed conflict. The spatial distribution of clusters aligns with known geopolitical hotspots, yet also uncovers less commonly studied conflict zones such as southern Mexico, northeastern India, and southeastern Nigeria, reaffirming the limitations of single-event-based conflict analyses. The concentration of clusters in sub-Saharan Africa and Latin America corresponds with findings from the literature, which identify both regions as increasingly affected by localized insurgencies, criminal networks, and climate-aggravated grievances [85]. The temporal profiles of the regional indicators also align with historical turning points. The Middle East's sharp post-2011 escalation reflects the onset of the Arab Spring and subsequent civil wars in Syria, Libya, and Yemen [86], whereas the late-2010s rise in Latin American intra-connectivity and average intensity, reflecting the instability of conflict area and linkage of conflicts, matches the post-accord fragmentation and narco-political restructuring in Colombia [87]. The continuous increase in sub-Saharan Africa corresponds with the expansion of jihadist insurgencies and growing inter-communal tensions in the Sahel and Horn of Africa [88]. The findings for South Asia and Afghanistan exemplify Walter's [89] "conflict trap" paradigm, where persistent high-frequency, dispersion, and intra-connectivity metrics reflect self-reinforcing violence mechanisms through refugee flows and arms trafficking.

A central finding across all four cluster-level indicators is the persistent dominance of structural variables, particularly those related to historical conflict exposure, socio-economic exclusion, and spatial marginalization. The dominance of historical conflict exposure across all outcome variables aligns with the theory of conflict persistence and path dependency, as proposed by Walter [90], who argues that the institutional legacies of violence increase the likelihood of recurring conflict due to weakened governance structures, loss of trust, and mobilization inertia. This is further supported by empirical work such as that by Collier et al. [91], who identified previous civil war as one of the most robust predictors of renewed conflict. The high relevance of vegetation coverage (NDVI) and topographical features (e.g., distance to border or capital) echoes findings in the environmental security literature, where resource abundance and geographic access are shown to facilitate armed group activity. For instance, Buhaug and Rød [92] demonstrated that forest cover and remoteness significantly predict civil war onset in sub-Saharan Africa. The spatial enablers of violence, such as border proximity, also align with theories of conflict diffusion and transnational contagion, as discussed by Buhaug and Gleditsch [33] and Schutte and Weidmann [27], who emphasize the role of porous borders and regional networks in facilitating violence escalation. The moderate contribution of climate anomalies (SPI and STI) suggests that environmental stressors alone are not sufficient to trigger conflict. This finding aligns with recent meta-analyses [38,93], which show that while climate variability can act as a threat multiplier, its effects are typically contingent on socio-political context, including weak institutions and economic marginalization [35]. Socio-economic variables, including GDP, population density, infant mortality, and ethnic diversity, also contributed significantly, supporting long-standing hypotheses in conflict research that link horizontal inequalities [94] and development gaps [95] to elevated conflict risk.

Spatial patterns observed in four conflict indicators—the number of conflicts, average intensity, dispersion, and intra-connectivity—highlight regional differences in temperature and precipitation anomalies in shaping armed conflict dynamics. These findings reveal how climate stress selectively affects different aspects of conflict systems, often depending on local environmental and institutional conditions. In regions like South Asia and the Middle East, STI and SPI exert a compound influence; West African zones exhibit similar dual climate stress, consistent with previous studies. Burke et al. [96,97] found a link between temperature and civil war in sub-Saharan Africa during 1981–2002; Miguel et al. [98] also found a link between negative rainfall bias and increased risk of civil war in Africa, and that water scarcity can lead to conflict behavior, especially in poor areas; Raleigh and Kniveton and Theisen [99,100] found that community conflict is most likely to occur during or after the rainy season. In Myanmar or Libya, for example, our study found that STI had a greater impact on all conflict indicators, suggesting heat stress as the primary climatic force for conflict propagation and intensification. This corroborates findings where excessive temperature correlates with unrest through physiological stress or reduced productivity [70]. In precipitation-dominated regions like Kenya and Nepal, previous work suggests that rainfall variability disrupts livelihoods and increases the likelihood of insurgent recruitment or communal clashes, especially in areas lacking adaptive capacity [101]. However, the influence of climate on each index is asymmetric, which indicates that different indexes in different regions have different sensitivity to temperature and precipitation anomalies. The differentiated response of intra-connectivity versus frequency in Mexico and Guatemala, for example, suggests that not all dimensions of conflict are uniformly sensitive to the same climate variables. These dynamics align with recent network-based analyses emphasizing conflict "contagion" mechanisms, where precipitation shapes spatial synchronization of violence more than initial ignition [102].

5. Conclusions

By integrating network-based cluster detection with explainable machine learning, this study advances a multi-scalar understanding of armed conflict and highlights the heterogeneity of different drivers. Using Random Forests and SHAP analysis, we found that historical exposure, socio-economic deprivation, and spatial structure are the primary determinants of conflict patterns. While climatic variables contribute less prominently, they remain relevant as part of a broader system of environmental vulnerability. This study highlights regionally distinct patterns of climate–conflict linkage by mapping the spatial responses of four structural conflict indicators to STI and SPI anomalies. Areas such as northern South Asia, Syria–Iraq, and Colombia demonstrate compound climate drivers across multiple conflict dimensions, while other regions are selectively sensitive to either heat or precipitation extremes.

From a policy perspective, our findings emphasize the need for targeted prevention strategies that account not only for environmental risks but also for entrenched inequalities and historical conflict legacies. Spatially aware interventions—particularly in border zones and ethnically fragmented regions—are crucial for mitigating both the spread and severity of future conflict. Indicator-specific climate sensitivities further underscore the need to tailor conflict risk assessments to local climatic and structural profiles. These findings underscore the need for region-specific policy interventions, particularly in climate-sensitive zones, and support calls for adaptive governance frameworks that consider both spatial clustering and climatic stress using targeted resource allocation to strengthen local resilience. While this study contributes novel insights, several limitations must be acknowledged. First, the temporal resolution of SPI and STI may not fully capture short-term weather shocks that could influence acute violence. Second, SHAP analysis, while interpretable, assumes

additive feature contribution and may oversimplify variable interactions. Future work could explore nonlinear interaction effects between variables using ensemble or deep learning methods, or extend the framework by incorporating temporal dynamics, sub-national political indicators, and interactive effects between variables to further unravel the complex causal pathways leading to violence.

Supplementary Materials: The following supporting information can be downloaded at: https://www.mdpi.com/article/10.3390/systems13080670/s1, Figures S1–S14: The spatial heterogeneity of the impact of other driving variables on armed conflict clusters; Figure S15: Correlation coefficient matrix of covariates; Figures S16–S19: Partial dependence plot of all variables for four outcome variables.

Author Contributions: Conceptualization, M.H., S.M. and J.W.; methodology, M.H., S.M. and J.W.; software, S.M.; validation, J.Z. and S.C.; formal analysis, J.W.; investigation, F.D.; resources, J.W., G.W. and J.D.; data curation, S.M. and J.W.; writing—original draft preparation, M.H., S.M. and D.J.; writing—review and editing, M.H., S.M. and J.W.; visualization, S.M. and J.W.; supervision, G.W. and J.D.; project administration, J.Z.; funding acquisition, M.H.; J.W. provided data related to the conflict, while G.W. and J.D. provided data on various driving factors as well as computational resources. All authors have read and agreed to the published version of the manuscript.

Funding: This work was funded by the Youth Innovation Promotion Association (Grant No. 2023000117).

Institutional Review Board Statement: Not applicable.

Informed Consent Statement: Not applicable.

Data Availability Statement: The raw data supporting the conclusions of this article will be made available by the authors on request.

Conflicts of Interest: The authors declare no conflicts of interest.

Abbreviations

The following abbreviations are used in this manuscript:

GDP	Gross domestic product
UCDP	Uppsala Conflict Data Program
WOPR	WorldPop Open Population Repository
SEDAC	Socioeconomic Data and Applications Center
GERG	Geo-referencing of ethnic groups
NDVI	Normalized Difference Vegetation Index
DAAC	Distributed Active Archive Center
AVHRR	Advanced Very-High-Resolution Radiometer
GRIP	Global Roads Inventory Project
CI	Critical infrastructure
GMBA	Global Mountain Biodiversity Assessment
NCAS	National Centre for Atmospheric Sciences
GHCN	Global Historical Climatology Network
RF	Random Forest regression
SHAP	SHapley Additive Explanations
SPI	Standardized precipitation index
STI	Standardized temperature index

Appendix A

Table A1. Sensitivity analysis on three cluster detection methods. We perform a sensitivity analysis on resolution parameter ($\gamma \in \{0.1, 1.0, 10, 100\}$) to test its impact on community granularity and modularity. If resolution is less than 1, modularity favors larger communities. Greater than 1 favors smaller communities. Communities are the number of communities; Min, Mean, Median, Max are the minimum, average, median, and maximum values of the number of grids in the formed community, respectively.

Method	Resolution	Communities	Min	Mean	Median	Max	Modularity
Greedy Modularity Optimization	0	98	1	55.86	4	1234	0.15
	1	107	1	51.16	4	808	0.28
	10	181	1	30.24	2	538	0.12
	100	357	1	15.33	1	277	0.07
Louvain Community Detection	0	225	1	24.33	6	226	0.18
	1	228	1	24.01	6	226	0.27
	10	289	1	18.94	3	278	0.12
	100	458	1	11.95	2	213	0.07
Asynchronous Label Propagation	-	610	1	8.97	1	228	0.15

References

1. Kurecic, P. Geoeconomic and Geopolitical Conflicts: Outcomes of the Geopolitical Economy in a Contemporary World. *World Rev. Political Econ.* **2015**, *6*, 522–543. [CrossRef]
2. Sundberg, R.; Melander, E. Introducing the UCDP Georeferenced Event Dataset. *J. Peace Res.* **2013**, *50*, 523–532. [CrossRef]
3. Li, A.; Yang, Y.; Li, M.; Niu, L. Research on the Spatiotemporal Evolution Characteristics of Armed Conflicts in Africa from 1989 to 2021. *World Reg. Stud.* **2024**, *33*, 18. [CrossRef]
4. Ugwu, C.N.; Ugwu, O.P.-C.; Alum, E.U.; Eze, V.H.U.; Basajja, M.; Ugwu, J.N.; Ogenyi, F.C.; Ejemot-Nwadiaro, R.I.; Okon, M.B.; Egba, S.I.; et al. Sustainable Development Goals (SDGs) and Resilient Healthcare Systems: Addressing Medicine and Public Health Challenges in Conflict Zones. *Medicine* **2025**, *104*, e41535. [CrossRef] [PubMed]
5. Collier, P. On the Economic Consequences of Civil War. *Oxf. Econ. Pap.* **1999**, *51*, 168–183. [CrossRef]
6. Rajmil, D.; Morales, L. The Role of Geopolitical Risk in Conflict Analysis: Critical Insights. *Peace Rev.* **2023**, *35*, 603–613. [CrossRef]
7. Camargo, G.; Sampayo, A.M.; Peña Galindo, A.; Escobedo, F.J.; Carriazo, F.; Feged-Rivadeneira, A. Exploring the Dynamics of Migration, Armed Conflict, Urbanization, and Anthropogenic Change in Colombia. *PLoS ONE* **2020**, *15*, e0242266. [CrossRef]
8. Cederman, L.-E.; Weidmann, N.B.; Gleditsch, K.S. Horizontal Inequalities and Ethnonationalist Civil War: A Global Comparison. *Am. Political Sci. Rev.* **2011**, *105*, 478–495. [CrossRef]
9. Stephenne, N. Analyzing Spatial Drivers in Quantitative Conflict Studies: The Potential and Challenges of Geographic Information Systems. *Int. Stud. Rev.* **2009**, *11*, 502–522. [CrossRef]
10. Cantillo, T.; Garza, N. Armed Conflict, Institutions and Deforestation: A Dynamic Spatiotemporal Analysis of Colombia 2000–2018. *World Dev.* **2022**, *160*, 106041. [CrossRef]
11. Johnson, D.; Toft, M. Grounds for War: The Evolution of Territorial Conflict. *Int. Secur.* **2013**, *38*, 7–38. [CrossRef]
12. Raleigh, C. Political Hierarchies and Landscapes of Conflict across Africa. *Political Geogr.* **2014**, *42*, 92–103. [CrossRef]
13. Ge, Q.; Hao, M.; Ding, F.; Jiang, D.; Scheffran, J.; Helman, D.; Ide, T. Modelling Armed Conflict Risk under Climate Change with Machine Learning and Time-Series Data. *Nat. Commun.* **2022**, *13*, 2839. [CrossRef]
14. Wang, Q.; Hao, M.; Helman, D.; Ding, F.; Jiang, D.; Xie, X.; Chen, S.; Ma, T. Quantifying the Influence of Climate Variability on Armed Conflict in Africa, 2000–2015. *Environ. Dev. Sustain.* **2023**, *25*, 9289–9306. [CrossRef]
15. Madu, I.A.; Nwankwo, C.F. Spatial Pattern of Climate Change and Farmer–Herder Conflict Vulnerabilities in Nigeria. *GeoJournal* **2021**, *86*, 2691–2707. [CrossRef]
16. Ide, T. Rise or Recede? How Climate Disasters Affect Armed Conflict Intensity. *Int. Secur.* **2023**, *47*, 50–78. [CrossRef]
17. Scartozzi, C.M. Reframing Climate-Induced Socio-Environmental Conflicts: A Systematic Review. *Int. Stud. Rev.* **2021**, *23*, 696–725. [CrossRef]
18. Collier, P. Greed and Grievance in Civil War. *Oxf. Econ. Pap.* **2004**, *56*, 563–595. [CrossRef]
19. Hegre, H.; Ellingsen, T.; Gates, S.; Gleditsch, N.P. Toward a Democratic Civil Peace? Democracy, Political Change, and Civil War, 1816–1992. *Am. Political Sci. Rev.* **2001**, *95*, 33–48. [CrossRef]
20. Nordås, R.; Gleditsch, N.P. Climate Change and Conflict. *Political Geogr.* **2007**, *26*, 627–638. [CrossRef]
21. Tollefsen, A.F.; Strand, H.; Buhaug, H. PRIO-GRID: A Unified Spatial Data Structure. *J. Peace Res.* **2012**, *49*, 363–374. [CrossRef]

22. Mjelva, M.B. *Rainfall Variability and Violent, State-Based Conflict*; Department of Political Science University of Oslo: Oslo, Norway, 2020.
23. Hegre, H.; Karlsen, J.; Nygård, H.M.; Strand, H.; Urdal, H. Predicting Armed Conflict, 2010–2050[1]. *Int. Stud. Q.* **2013**, *57*, 250–270. [CrossRef]
24. Trinn, C.; Wencker, T. Integrating the Quantitative Research on the Onset and Incidence of Violent Intrastate Conflicts. *Int. Stud. Rev.* **2021**, *23*, 115–139. [CrossRef]
25. Buhaug, H.; Lujala, P. Accounting for Scale: Measuring Geography in Quantitative Studies of Civil War. *Political Geogr.* **2005**, *24*, 399–418. [CrossRef]
26. Guha-Sapir, D.; Van Panhuis, W.G. Conflict-related Mortality: An Analysis of 37 Datasets. *Disasters* **2004**, *28*, 418–428. [CrossRef]
27. Schutte, S.; Weidmann, N.B. Diffusion Patterns of Violence in Civil Wars. *Political Geogr.* **2011**, *30*, 143–152. [CrossRef]
28. Kumarihamy, R.M.K.; Shahnawaz, A.S.L.; Tripathi, T.N.K. Spatio-Temporal Patterns of Armed Conflicts in Sri Lanka: 1989–2016. *Trans. Inst. Indian Geogr.* **2020**, *42*, 47.
29. Maswanganye, M. *Spatial and Temporal Patterns of Conflict Events in Africa: An Exploratory Analysis*; University of the Witwatersrand: Johannesburg, South Africa, 2018.
30. Kibris, A. The Geo-Temporal Evolution of Violence in Civil Conflicts: A Micro Analysis of Conflict Diffusion on a New Event Data Set. *J. Peace Res.* **2021**, *58*, 885–899. [CrossRef]
31. Tadesse, H. Modelling Conflict Dynamics: Evidence from Africa: What Do the Data Show via Spatiotemporal Global ACLED Dataset? *Appl. Spat. Anal. Policy* **2023**, *16*, 1541–1559. [CrossRef]
32. Oliveros, D.A.V.; Koren, O. Measuring Spatio-Temporal Civil War Dimensions Using Community-Based Dynamic Network Representation (CoDNet). *IEEE Trans. Comput. Soc. Syst.* **2023**, *11*, 1506–1516. [CrossRef]
33. Buhaug, H.; Gleditsch, K.S. Contagion or Confusion? Why Conflicts Cluster in Space. *Int. Stud. Q.* **2008**, *52*, 215–233. [CrossRef]
34. Masrur, A.; Yu, M.; Mitra, P.; Peuquet, D.; Taylor, A. Interpretable Machine Learning for Analysing Heterogeneous Drivers of Geographic Events in Space-Time. *Int. J. Geogr. Inf. Sci.* **2021**, *36*, 692–719. [CrossRef]
35. Hao, M.; Ding, F.; Xie, X.; Fu, J.; Qian, Y.; Ide, T.; Maystadt, J.-F.; Chen, S.; Ge, Q.; Jiang, D. Varying Climatic-Social-Geographical Patterns Shape the Conflict Risk at Regional and Global Scales. *Humanit. Soc. Sci. Commun.* **2022**, *9*, 276. [CrossRef]
36. Zhang, Y.; Liu, Y.; Zhang, Y.; Kong, X.; Jing, Y.; Cai, E.; Zhang, L.; Liu, Y.; Wang, Z.; Liu, Y. Spatial Patterns and Driving Forces of Conflicts among the Three Land Management Red Lines in China: A Case Study of the Wuhan Urban Development Area. *Sustainability* **2019**, *11*, 2025. [CrossRef]
37. Cappelli, F.; Castronuovo, G.; Grimaldi, S.; Telesca, V. Random Forest and Feature Importance Measures for Discriminating the Most Influential Environmental Factors in Predicting Cardiovascular and Respiratory Diseases. *Int. J. Environ. Res. Public Health* **2024**, *21*, 867. [CrossRef]
38. Burke, M.; Hsiang, S.M.; Miguel, E. Climate and Conflict. *Annu. Rev. Econ.* **2015**, *7*, 577–617. [CrossRef]
39. Hegre, H.; Allansson, M.; Basedau, M.; Colaresi, M.; Croicu, M.; Fjelde, H.; Hoyles, F.; Hultman, L.; Högbladh, S.; Jansen, R.; et al. ViEWS: A Political Violence Early-Warning System. *J. Peace Res.* **2019**, *56*, 155–174. [CrossRef]
40. Besley, T.; Reynal-Querol, M. The Legacy of Historical Conflict: Evidence from Africa. *Am. Polit. Sci. Rev.* **2014**, *108*, 319–336. [CrossRef]
41. Chen, J.; Gao, M.; Cheng, S.; Hou, W.; Song, M.; Liu, X.; Liu, Y. Global 1 Km × 1 Km Gridded Revised Real Gross Domestic Product and Electricity Consumption during 1992–2019 Based on Calibrated Nighttime Light Data. *Sci. Data* **2022**, *9*, 202. [CrossRef]
42. Goldstone, J.A. Population and Security: How Demographic Change Can Lead to Violent Conflict. *J. Int. Aff.* **2002**, *56*, 3–21.
43. WorldPop. Global 1km Population. Available online: https://hub.worldpop.org/project/categories?id=3 (accessed on 3 June 2025).
44. Garry, S.; Checchi, F. Armed Conflict and Public Health: Into the 21st Century. *J. Public Health* **2020**, *42*, e287–e298. [CrossRef]
45. Yuan, B.; Wang, Z.; Li, J. Social Vulnerability and Infant Mortality in Space Dimension: An Investigation of the World's Most Underdeveloped West Africa Coastal Area. *Int. J. Hum. Rights Healthc.* **2020**, *13*, 239–248. [CrossRef]
46. Earth Science Data Systems, N. SEDAC | NASA Earthdata. Available online: https://www.earthdata.nasa.gov/centers/sedac-daac (accessed on 28 April 2025).
47. Bleaney, M.; Dimico, A. Ethnic Diversity and Conflict. *J. Institutional Econ.* **2017**, *13*, 357–378. [CrossRef]
48. Montalvo, J.G.; Reynal-Querol, M. Ethnic Polarization, Potential Conflict, and Civil Wars. *Am. Econ. Rev.* **2005**, *95*, 796–816. [CrossRef]
49. Weidmann, N.B.; Rød, J.K.; Cederman, L.-E. Representing Ethnic Groups in Space: A New Dataset. *J. Peace Res.* **2010**, *47*, 491–499. [CrossRef]
50. Le Billon, P. Resources and Armed Conflicts. *Adelphi Pap.* **2005**, *45*, 29–49. [CrossRef]
51. Maus, V.; Giljum, S.; da Silva, D.M.; Gutschlhofer, J.; da Rosa, R.P.; Luckeneder, S.; Gass, S.L.B.; Lieber, M.; McCallum, I. An Update on Global Mining Land Use. *Sci. Data* **2022**, *9*, 433. [CrossRef]

52. Eastin, J. Fuel to the Fire: Natural Disasters and the Duration of Civil Conflict. *Int. Interact.* **2016**, *42*, 322–349. [CrossRef]
53. Nel, P.; Righarts, M. Natural Disasters and the Risk of Violent Civil Conflict. *Int. Stud. Q.* **2008**, *52*, 159–185. [CrossRef]
54. Agwe, J.N.; Arnold, M.; Buys, P.; Chen, R.S.; Deichmann, U.K.; Dilley, M.; Kjevstad, O.; Lerner-Lam, A.L.; Lyon, B.; Yetman, G. *Natural Disaster Hotspots: A Global Risk Analysis*; World Bank: Washington, DC, USA, 2005.
55. Meier, P.; Bond, D.; Bond, J. Environmental Influences on Pastoral Conflict in the Horn of Africa. *Political Geogr.* **2007**, *26*, 716–735. [CrossRef]
56. Pinzon, J.E.; Pak, E.W.; Tucker, C.J.; Bhatt, U.S.; Frost, G.V.; Macander, M.J. Vegetation CollectionGlobal Vegetation Greenness (NDVI) from AVHRR GIMMS-3G+, 1981–2022. 2023. Available online: https://daac.ornl.gov/VEGETATION/guides/Global_Veg_Greenness_GIMMS_3G.html (accessed on 3 June 2025).
57. Zhukov, Y.M. Roads and the Diffusion of Insurgent Violence: The Logistics of Conflict in Russia's North Caucasus. *Political Geogr.* **2012**, *31*, 144–156. [CrossRef]
58. Meijer, J.R.; Huijbregts, M.A.J.; Schotten, K.C.G.J.; Schipper, A.M. Global Patterns of Current and Future Road Infrastructure. *Environ. Res. Lett.* **2018**, *13*, 064006. [CrossRef]
59. Winkler, K.; Fuchs, R.; Rounsevell, M.; Herold, M. Global Land Use Changes Are Four Times Greater than Previously Estimated. *Nat. Commun.* **2021**, *12*, 2501. [CrossRef]
60. Nirandjan, S.; Koks, E.E.; Ward, P.J.; Aerts, J.C.J.H. A Spatially-Explicit Harmonized Global Dataset of Critical Infrastructure. *Sci. Data* **2022**, *9*, 150. [CrossRef]
61. Carter, D.B.; Shaver, A.C.; Wright, A.L. Places to Hide: Terrain, Ethnicity, and Civil Conflict. *J. Politics* **2019**, *81*, 1446–1465. [CrossRef]
62. Snethlage, M.A.; Geschke, J.; Ranipeta, A.; Jetz, W.; Yoccoz, N.G.; Körner, C.; Spehn, E.M.; Fischer, M.; Urbach, D. A Hierarchical Inventory of the World's Mountains for Global Comparative Mountain Science. *Sci. Data* **2022**, *9*, 149. [CrossRef]
63. Hendrix, C.S.; Salehyan, I. Climate Change, Rainfall, and Social Conflict in Africa. *J. Peace Res.* **2012**, *49*, 35–50. [CrossRef]
64. van Weezel, S. On Climate and Conflict: Precipitation Decline and Communal Conflict in Ethiopia and Kenya. *J. Peace Res.* **2019**, *56*, 514–528. [CrossRef]
65. Habibi, N. *Conflict in Ethiopia: The Impact of Precipitation and Its Transmission Mechanism*; HiCN Working Papers; Households in Conflict Network: Berlin, Germany, 2017; No 248.
66. Harris, I.; Osborn, T.J.; Jones, P.; Lister, D. Version 4 of the CRU TS Monthly High-Resolution Gridded Multivariate Climate Dataset. *Sci. Data* **2020**, *7*, 109. [CrossRef]
67. Breckner, M.; Sunde, U. Temperature Extremes, Global Warming, and Armed Conflict: New Insights from High Resolution Data. *World Dev.* **2019**, *123*, 104624. [CrossRef]
68. Guo, Y.; Gao, Y.; He, C.; Zhu, Y.; Zhou, L.; Kan, H.; Chen, R. Short-Term High Temperature May Increase the Incidence Risk of Collective Conflicts: A Case-Crossover Study in the Greater Middle East. *Sci. Total Environ.* **2024**, *915*, 170105. [CrossRef]
69. Helman, D.; Zaitchik, B.F. Temperature Anomalies Affect Violent Conflicts in African and Middle Eastern Warm Regions. *Glob. Environ. Chang.* **2020**, *63*, 102118. [CrossRef]
70. Hsiang, S.M.; Burke, M.; Miguel, E. Quantifying the Influence of Climate on Human Conflict. *Science* **2013**, *341*, 1235367. [CrossRef]
71. Fan, Y.; Van Den Dool, H. A Global Monthly Land Surface Air Temperature Analysis for 1948–Present. *J. Geophys. Res.* **2008**, *113*, D01103. [CrossRef]
72. Basnet, S. Analysis of Social Unrest Events Using Spatio-Temporal Data Clustering and Agent-Based Modelling. Department of Computer Science and Engineering: Dissertations, Theses, and Student Research. Master's Thesis, University of Nebraska-Lincoln, Lincoln, NE, USA, 2019.
73. Sehgal, G.; Sharma, K.; Chatterjee, A.; Chakraborti, A. Spatio-Temporal Networks of Social Conflicts: Analysis and Modeling. In Proceedings of the 2018 IEEE/ACM International Conference on Advances in Social Networks Analysis and Mining, Barcelona, Spain, 28–31 August 2018; IEEE Press: Piscataway, NJ, USA, 2018; pp. 740–743.
74. Wu, J. Analysis and Spatio-Temporal Simulation of Diffusion Characteristics of Geo-Conflict Events. Ph.D. Thesis, University of Chinese Academy of Sciences, Beijing, China, 2024.
75. Lee, E.D.; Daniels, B.C.; Myers, C.R.; Krakauer, D.C.; Flack, J.C. Scaling Theory of Armed-Conflict Avalanches. *Phys. Rev. E* **2020**, *102*, 042312. [CrossRef]
76. Raleigh, C.; Hegre, H. Population Size, Concentration, and Civil War. A Geographically Disaggregated Analysis. *Political Geogr.* **2009**, *28*, 224–238. [CrossRef]
77. Blondel, V.D.; Guillaume, J.-L.; Lambiotte, R.; Lefebvre, E. Fast Unfolding of Communities in Large Networks. *J. Stat. Mech.* **2008**, *2008*, P10008. [CrossRef]
78. Dugué, N.; Perez, A. *Directed Louvain: Maximizing Modularity in Directed Networks*; Université d'Orléans: Orléans, France, 2015.
79. Traag, V.A.; Waltman, L.; van Eck, N.J. From Louvain to Leiden: Guaranteeing Well-Connected Communities. *Sci. Rep.* **2019**, *9*, 5233. [CrossRef]

80. Singha, S.P.; Hossain, M.M.; Rahman, M.A.; Sharmin, N. Investigation of Graph-Based Clustering Approaches along with Graph Neural Networks for Modeling Armed Conflict in Bangladesh. *Int. J. Data Sci.* **2024**, *18*, 187–203. [CrossRef]
81. Oh, W.; Muneepeerakul, R.; Rubenstein, D.; Levin, S. Emergent Network Patterns of Internal Displacement in Somalia Driven by Natural Disasters and Conflicts. *Glob. Environ. Chang.* **2024**, *84*, 102793. [CrossRef]
82. Yue, H.; Chen, J. Interpretable Spatial Machine Learning for Understanding Spatial Heterogeneity in Factors Affecting Street Theft Crime. *Appl. Geogr.* **2025**, *175*, 103503. [CrossRef]
83. Oshiro, T.M.; Perez, P.S.; Baranauskas, J.A. How Many Trees in a Random Forest? In Proceedings of the Machine Learning and Data Mining in Pattern Recognition; Perner, P., Ed.; Springer: Berlin/Heidelberg, Germany, 2012; pp. 154–168.
84. Lundberg, S.M.; Lee, S.-I. A Unified Approach to Interpreting Model Predictions. In Proceedings of the 31st International Conference on Neural Information Processing Systems, Long Beach, CA, USA, 4–9 December 2017; Curran Associates Inc.: Red Hook, NY, USA, 2017; pp. 4768–4777.
85. Matsuo, T.; Schmidt, T.S. Managing Tradeoffs in Green Industrial Policies: The Role of Renewable Energy Policy Design. *World Dev.* **2019**, *122*, 11–26. [CrossRef]
86. Ahram, A.I. *War and Conflict in the Middle East and North Africa*; John Wiley & Sons: Hoboken, NJ, USA, 2020; ISBN 978-1-5095-3284-1.
87. Richani, N. The Political Economy of Violence: The War-System in Colombia. *J. Interam. Stud. World Aff.* **1997**, *39*, 37–81. [CrossRef]
88. Brown, O.; Hammill, A.; McLeman, R. Climate Change as the "New" Security Threat: Implications for Africa. *Int. Aff.* **2007**, *83*, 1141–1154. [CrossRef]
89. Walter, B.F. Why Bad Governance Leads to Repeat Civil War. *J. Confl. Resolut.* **2015**, *59*, 1242–1272. [CrossRef]
90. Walter, B.F. Does Conflict Beget Conflict? Explaining Recurring Civil War. *J. Peace Res.* **2004**, *41*, 371–388. [CrossRef]
91. Collier, P.; Hoeffler, A.; Söderbom, M. On the Duration of Civil War. *J. Peace Res.* **2004**, *41*, 253–273. [CrossRef]
92. Buhaug, H.; Rød, J.K. Local Determinants of African Civil Wars, 1970–2001. *Political Geogr.* **2006**, *25*, 315–335. [CrossRef]
93. Mach, K.J.; Kraan, C.M.; Adger, W.N.; Buhaug, H.; Burke, M.; Fearon, J.D.; Field, C.B.; Hendrix, C.S.; Maystadt, J.-F.; O'Loughlin, J.; et al. Climate as a Risk Factor for Armed Conflict. *Nature* **2019**, *571*, 193–197. [CrossRef]
94. Stewart, F. Horizontal Inequalities and Conflict: An Introduction and Some Hypotheses. In *Horizontal Inequalities and Conflict: Understanding Group Violence in Multiethnic Societies*; Stewart, F., Ed.; Palgrave Macmillan: London, UK, 2008; pp. 3–24, ISBN 978-0-230-58272-9.
95. Fearon, J.D.; Laitin, D.D. Ethnicity, Insurgency, and Civil War. *Am. Political Sci. Rev.* **2003**, *97*, 75–90. [CrossRef]
96. Burke, M.B.; Miguel, E.; Satyanath, S.; Dykema, J.A.; Lobell, D.B. Warming Increases the Risk of Civil War in Africa. *Proc. Natl. Acad. Sci. USA* **2009**, *106*, 20670–20674. [CrossRef]
97. Burke, M.B.; Miguel, E.; Satyanath, S.; Dykema, J.A.; Lobell, D.B. Climate Robustly Linked to African Civil War. *Proc. Natl. Acad. Sci. USA* **2010**, *107*, E185. [CrossRef]
98. Miguel, E.; Satyanath, S.; Sergenti, E. Economic Shocks and Civil Conflict: An Instrumental Variables Approach. *J. Political Econ.* **2004**, *112*, 725–753. [CrossRef]
99. Raleigh, C.; Kniveton, D. Come Rain or Shine: An Analysis of Conflict and Climate Variability in East Africa. *J. Peace Res.* **2012**, *49*, 51–64. [CrossRef]
100. Theisen, O.M. Climate Clashes? Weather Variability, Land Pressure, and Organized Violence in Kenya, 1989–2004. *J. Peace Res.* **2012**, *49*, 81–96. [CrossRef]
101. Selby, J.; Hoffmann, C. (Eds.) *Rethinking Climate Change, Conflict and Security*; Routledge: London, UK, 2017; ISBN 978-1-315-69023-0.
102. Schleussner, C.-F.; Donges, J.F.; Donner, R.V.; Schellnhuber, H.J. Armed-Conflict Risks Enhanced by Climate-Related Disasters in Ethnically Fractionalized Countries. *Proc. Natl. Acad. Sci. USA* **2016**, *113*, 9216–9221. [CrossRef]

Disclaimer/Publisher's Note: The statements, opinions and data contained in all publications are solely those of the individual author(s) and contributor(s) and not of MDPI and/or the editor(s). MDPI and/or the editor(s) disclaim responsibility for any injury to people or property resulting from any ideas, methods, instructions or products referred to in the content.